

Microwave dielectric properties of ATiO_3 ($A = \text{Ni, Mg, Co, Mn}$) ceramics

Eung Soo Kim*, Chang Jun Jeon

Department of Materials Engineering, Kyonggi University, Suwon 443-760, Republic of Korea

Available online 6 September 2009

Abstract

Relationships between structural characteristics and microwave dielectric properties of ATiO_3 ($A = \text{Ni, Mg, Co, Mn}$) with ilmenite structure were investigated. The oxygen octahedral distortion was dependent on the type of A-site ions which affected to the temperature coefficient of the resonant frequency (TCF) of ATiO_3 ceramics. The quality factor (Qf) of ATiO_3 ($A = \text{Mn, Ni, Co}$) specimens was appreciably lowered than that of MgTiO_3 specimens due to the degree of covalency of cation–oxygen ion bond and the ordering of A-site ions. Also, the dielectric constant (K) was dependent on the electronic oxide polarizabilities of ATiO_3 ceramics.

© 2009 Elsevier Ltd. All rights reserved.

Keywords: Ilmenite structure; Dielectric properties; Covalency; Octahedral distortion; Electronic oxide polarizabilities

1. Introduction

ATiO_3 ($A = \text{Ni, Mg, Co, Mn}$) ceramics have the ilmenite structure, which is an ordered derivative of the corundum structure. The ilmenite structure is based on hexagonal closest packed oxygen layers with cations occupying two thirds of the octahedral sites available.¹ In contrast to the fully disordered corundum structure, the ilmenite structure results from equal amounts of divalent and tetravalent cations, which are ordered at the octahedral sites and alternate along the c -axis of the unit cell. The same type of octahedron in the ilmenite structure shares an edge along the a -axis, a pair of AO_6 and TiO_6 octahedra shares a face along the c -axis and a corner along the oblique direction. One pair of edge-shared TiO_6 octahedra is isolated by the cation vacancies along the a -axis and that is separated by the AO_6 octahedron along the oblique direction.

If the ionic radius of A-site ion is much larger than 1.0 \AA , such as Ca^{2+} (1.34 \AA) or Sr^{2+} (1.44 \AA)² in CaTiO_3 or SrTiO_3 , the compound turns to the perovskite structure which is formed by corner sharing of the TiO_6 octahedron, and the coordination number of A-site cations turns from 6 to 12.

For high frequency applications and stability of the resonant frequency, the low loss dielectric materials with ilmenite structure such as MgTiO_3 have been widely investigated for the microwave telecommunication systems.³ With the types of A-

site ions of ATiO_3 ceramics, the microwave dielectric properties are expected to be changed. Dependence of microwave dielectric properties on structural characteristics should be studied to control and predict the dielectric properties of ATiO_3 ilmenite compounds.

Therefore, the microwave dielectric properties of ilmenite titanates, ATiO_3 ($A = \text{Ni, Mg, Co, Mn}$) ceramics have been investigated in view point of the characteristics of bonds between cations and oxygen, the distortion of oxygen octahedra and ordering of cation in ilmenite structure.

2. Experimental procedure

ATiO_3 ($A = \text{Ni, Mg, Co, Mn}$) powders were separately prepared by a conventional solid-state reaction from oxide powders with purities above 99%. To obtain a single phase of each composition, ATiO_3 ($A = \text{Ni, Mg, Co, Mn}$) powders were calcined at 1100°C for 5 h. These calcined powders were milled again with ZrO_2 balls for 24 h in ethanol and then dried. The dried powders were pressed isostatically into 10 mm-diameter disks at 1500 kg/cm^2 . The resultant pellets were sintered from 1200 to 1500°C for 3 h in air.

The apparent densities of the sintered specimens were measured by Archimedes method. The relative densities were obtained from the apparent densities and the theoretical values. Powder X-ray diffraction (XRD) analyses (D/Max-3C, Rigaku, Japan) were used to determine the phase identification. The lattice parameters, unit cell volumes and atomic positions were obtained from Rietveld refinements of XRD patterns. The

* Corresponding author. Tel.: +82 31 249 9764; fax: +82 31 244 6300.
E-mail address: eskim@kyonggi.ac.kr (E.S. Kim).

Rietveld refinements were performed using the RIETAN-2000 program.⁴ The initial structure model for ilmenite compounds was taken from the work by Wechsler and Von Dreele,⁵ using neutron powder diffraction at room temperature. The ordering of crystal structure was confirmed by a Raman spectra meter (T 64000, HORIBA Jobin Yvon, France) with an Ar⁺ ion laser operating at 514 nm for excitation. The microstructure of the specimens was observed using a scanning electron microscope (SEM, JSM-6500F, JEOL, Japan). The microwave dielectric properties were measured by Hakki and Coleman's method⁶ with the TE₀₁₁ mode at 10–11 GHz. The TCF of specimens was measured by the cavity method⁷ in the temperature range from 25 to 80 °C.

3. Results and discussion

3.1. Physical properties

With the increase of sintering temperature from 1200 to 1500 °C, the sintered densities of ATiO₃ (A = Ni, Mg, Co, Mn) ceramics increased and showed the different sinterability with the types of A-site ions. To reduce the effects of density on the microwave dielectric properties, the optimal sintering temperatures for the higher sintered densities than 96% of theoretical values were 1300 °C for MnTiO₃, 1350 °C for MgTiO₃ and CoTiO₃, and 1400 °C for NiTiO₃, respectively.

Fig. 1 shows the XRD patterns of ATiO₃ (A = Ni, Mg, Co, Mn) sintered specimens. A single phase of the trigonal ilmenite structure (*R3-H*) was confirmed through the entire compositions. With the types of A-site ions (A = Ni, Mg, Co, Mn), the peak at $2\theta = 32^\circ\text{--}34^\circ$ in XRD patterns shifted to lower angle, which indicated that the unit cell volume increased with the ionic radius of A-site ions (A = Ni, Mg, Co, Mn). Since the ionic size of Ni²⁺ (0.69 Å) was smaller than those of Mg²⁺ (0.72 Å), Co²⁺ (0.745 Å) and Mn²⁺ (0.83 Å) at the same coordination number of 6,² the unit cell volume of NiTiO₃ specimens was smaller than those of MgTiO₃, CoTiO₃ and MnTiO₃ specimens. Also, the crystallographic parameters, refined atomic positions and occupancies of the sintered specimens obtained from the Rietveld refinement of XRD patterns are summarized in Table 1.

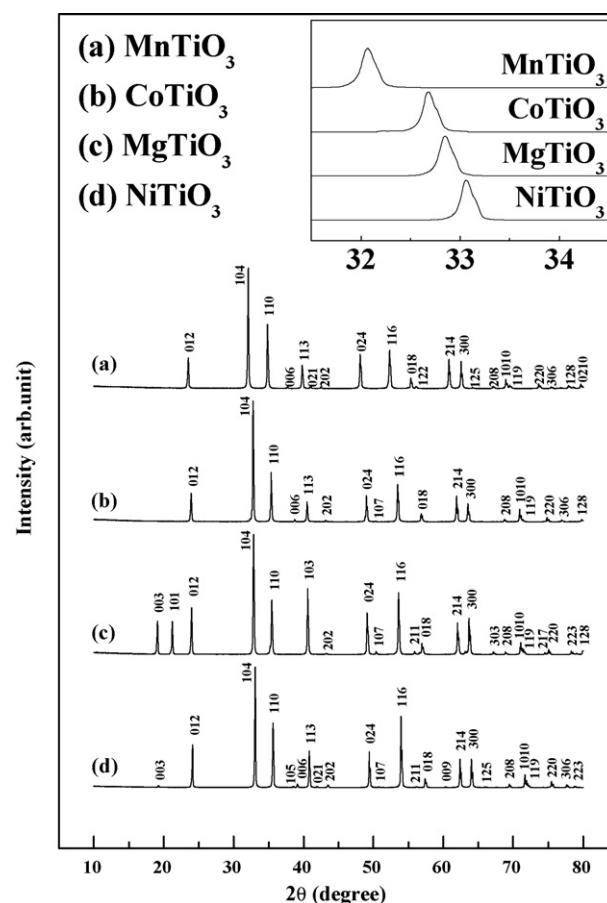


Fig. 1. X-ray diffraction patterns of ATiO₃ (A = Ni, Mg, Co, Mn) sintered specimens.

According to Pauling,⁸ the ionic character of bonds could be estimated by the electronegativity difference (Δe) between cation and oxygen by Eq. (1).

$$\Delta e = \frac{(X_{A-O} + X_{B-O})}{2} \quad (1)$$

Due to the larger electronegativity difference (Δe) than 2.0, MgTiO₃ (2.015) showed the larger ionic bond characteristics than NiTiO₃, CoTiO₃ and MnTiO₃ because those of NiTiO₃

Table 1
Crystallographic parameters, refined atomic positions and occupancies of ATiO₃ (A = Ni, Mg, Co, Mn) sintered specimens.

Compound	Atom	Wyckoff site	x	y	z	Occupation
NiTiO ₃	Ni	6c	0	0	0.3508	1.0
	Ti	6c	0	0	0.1440	1.0
	O	18f	0.3115	0.0057	0.2476	1.0
MgTiO ₃	Mg	6c	0	0	0.3557	1.0
	Ti	6c	0	0	0.1451	1.0
	O	18f	0.3159	0.0214	0.2463	1.0
CoTiO ₃	Co	6c	0	0	0.3551	1.0
	Ti	6c	0	0	0.1456	1.0
	O	18f	0.3162	0.0209	0.2459	1.0
MnTiO ₃	Mn	6c	0	0	0.3600	1.0
	Ti	6c	0	0	0.1476	1.0
	O	18f	0.3189	0.0310	0.2439	1.0

Table 2
Covalency of ATiO₃ (A = Ni, Mg, Co, Mn) sintered specimens.

Compound		R (Å)	R_1 (Å)	N	a	M	s	f_c	Covalency (%)	Average covalency (%)
MgTiO ₃	Mg–O	2.015	1.622	4.29	0.54	1.64	0.327	0.086	26.40	31.93
	Ti–O	1.977	1.806	5.20	0.49	1.57	0.624	0.234	37.46	
NiTiO ₃	Ni–O	2.049	1.680	5.40	0.60	1.50	0.342	0.120	35.09	35.61
	Ti–O	2.002	1.806	5.20	0.49	1.57	0.586	0.212	36.12	
CoTiO ₃	Co–O	2.111	1.727	5.60	0.60	1.50	0.325	0.111	34.20	35.83
	Ti–O	1.977	1.806	5.20	0.49	1.57	0.624	0.234	37.45	
MnTiO ₃	Mn–O	2.193	1.798	5.60	0.60	1.50	0.329	0.113	34.42	35.93
	Ti–O	1.978	1.806	5.20	0.49	1.57	0.624	0.233	37.44	

(1.715), CoTiO₃ (1.73) and MnTiO₃ (1.895) are smaller than 2.0. The bond characteristics between cation and oxygen of ATiO₃ (A = Ni, Mg, Co, Mn) could also be evaluated by the relationships between the bond strength (s) and covalency (f_c) of octahedral cation–oxygen ion bonds as shown in Eqs. (2)–(4).^{9,10}

$$s = \left(\frac{R}{R_1} \right)^{-N} \quad (2)$$

$$f_c = as^M \quad (3)$$

$$\text{Covalency (\%)} = \frac{f_c}{s} \times 100 \quad (4)$$

where R , R_1 and N are the refined bond length, empirical constant which depends on the cation site, and the constant which is different for each octahedral cation–oxygen ion pair, respectively. Moreover, a and M in Eq. (3) are empirical constants

which depend on the number of electrons. Table 2 summarizes the bond strength and covalency of ATiO₃ (A = Ni, Mg, Co, Mn) sintered specimens. Comparing to the covalency (%) of Mg–O bond of MgTiO₃, Ni–O, Co–O, and Mn–O bonds showed larger covalency (%) and Ti–O bonds of ATiO₃ did not changed much with the type of A-site ions. These results may be associated with the loss of electronic polarization of 3d electrons in Ni²⁺ (3d⁸), Co²⁺ (3d⁷) and Mn²⁺ (3d⁵).

SEM micrographs of ATiO₃ (A = Ni, Mg, Co, Mn) ceramics sintered at each optimal sintering temperature are shown in Fig. 2. The grain size of MnTiO₃ specimens was larger than those of ATiO₃ (A = Co, Ni, Mg) specimens.

3.2. Dielectric properties at microwave frequencies

Fig. 3 shows the dielectric constant (K) of ATiO₃ (A = Ni, Mg, Co, Mn) specimens sintered from 1200 to 1500 °C for 3 h.

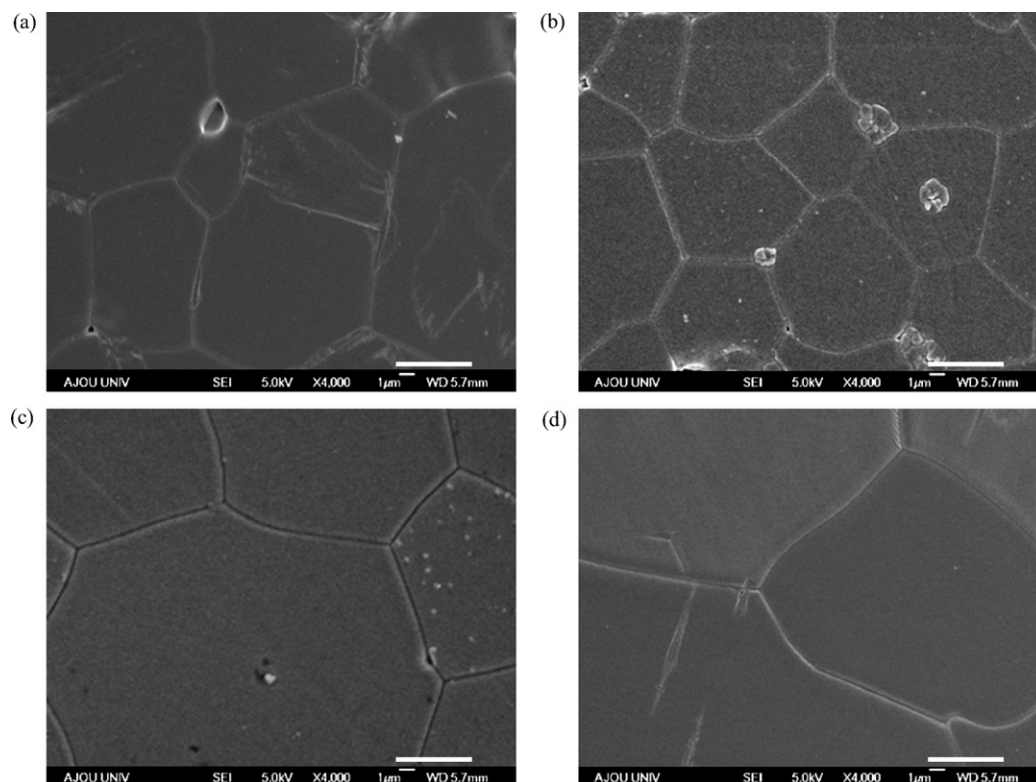


Fig. 2. SEM micrographs of ATiO₃ (A = Ni, Mg, Co, Mn) sintered specimens: (a) NiTiO₃, (b) MgTiO₃, (c) CoTiO₃, and (d) MnTiO₃ (bar = 5 μm).

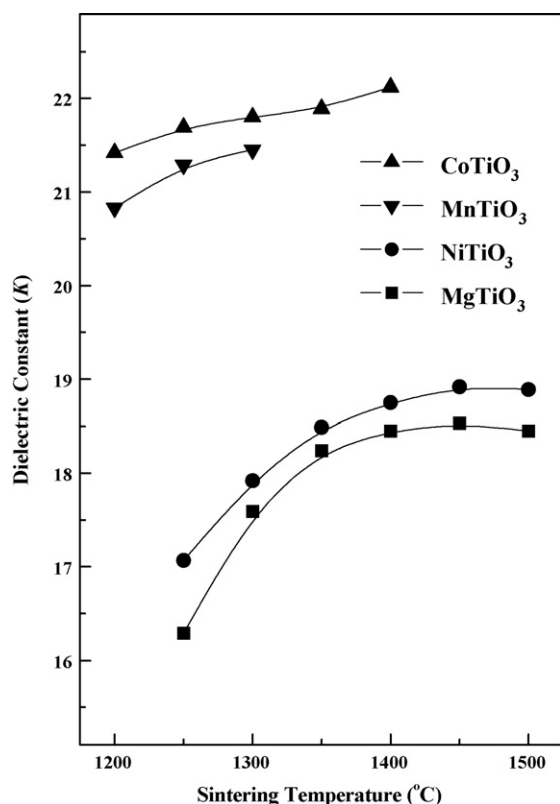


Fig. 3. Dielectric constant (K) of ATiO_3 ($A = \text{Ni, Mg, Co, Mn}$) specimens sintered from 1200 to 1500 °C for 3 h.

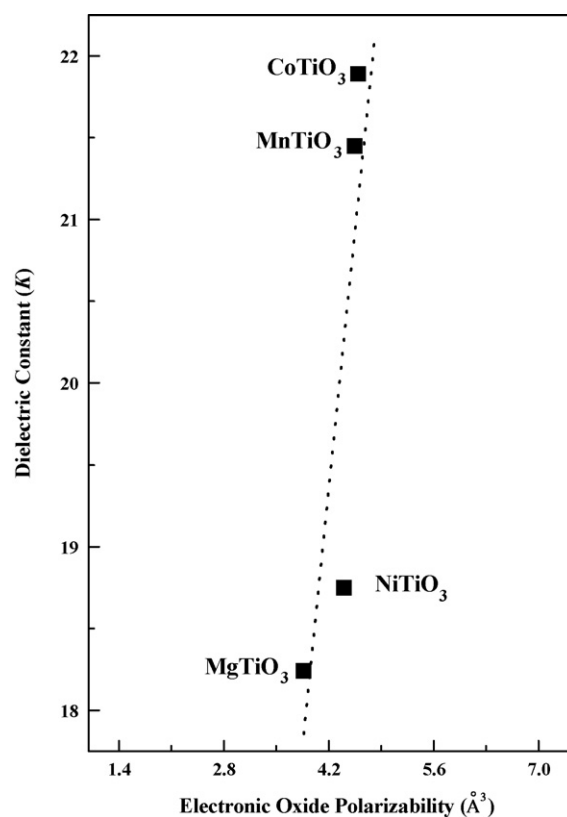


Fig. 4. Dependence of dielectric constant (K) on the electronic oxide polarizability of ATiO_3 ($A = \text{Ni, Mg, Co, Mn}$) sintered specimens.

With the increase of the sintering temperature, the K of the specimens was increased due to the increase of density. At microwave frequencies, the K is dependent on the theoretical dielectric polarizabilities ($\alpha_{\text{theo.}}$) obtained from the additive rule.¹¹ However, the K of CoTiO_3 was larger than those of MnTiO_3 , NiTiO_3 and MgTiO_3 , even though the $\alpha_{\text{theo.}}$ of MnTiO_3 (11.6 \AA^3) was larger than those of CoTiO_3 (10.61 \AA^3), MgTiO_3 (10.28 \AA^3) and NiTiO_3 (10.19 \AA^3). These results could be attributed to the bond characteristics of ATiO_3 ($A = \text{Ni, Mg, Co, Mn}$) ceramics. Due to the covalency of cation–oxygen bond and the localized 3d electrons Ni^{2+} (3d⁸), Co^{2+} (3d⁷) and Mn^{2+} (3d⁵), the electronic oxide polarizabilities ($\alpha_{\text{O}^{2-}}$) should be considered. The $\alpha_{\text{O}^{2-}}$ reported by Dimitrov and Sakka¹² from the energy gap and the molar volume as well as the polarizability of cation was used. With the ionic radius of A-site ions ($A = \text{Mg, Ni, Mn, Co}$), the K of the sintered specimens was increased due to the increase of the $\alpha_{\text{O}^{2-}}$, as shown in Fig. 4. Therefore, the energy gap and the molar volume should also be considered as well as the dielectric polarizabilities to predict and control the K of ATiO_3 with ilmenite structure.

Fig. 5 shows the quality factor (Qf) of ATiO_3 ($A = \text{Ni, Mg, Co, Mn}$) specimens sintered from 1200 to 1500 °C for 3 h. The Qf value of MgTiO_3 specimens was much larger than those of ($A = \text{Co, Ni, Mn}$) specimens. It has been reported¹¹ that the Qf value was dependent on density, secondary phase and grain size. In these systems, the effects of the density, secondary phase and grain size could be neglected, because the relative density was higher than 96%, and there was no secondary phase and no

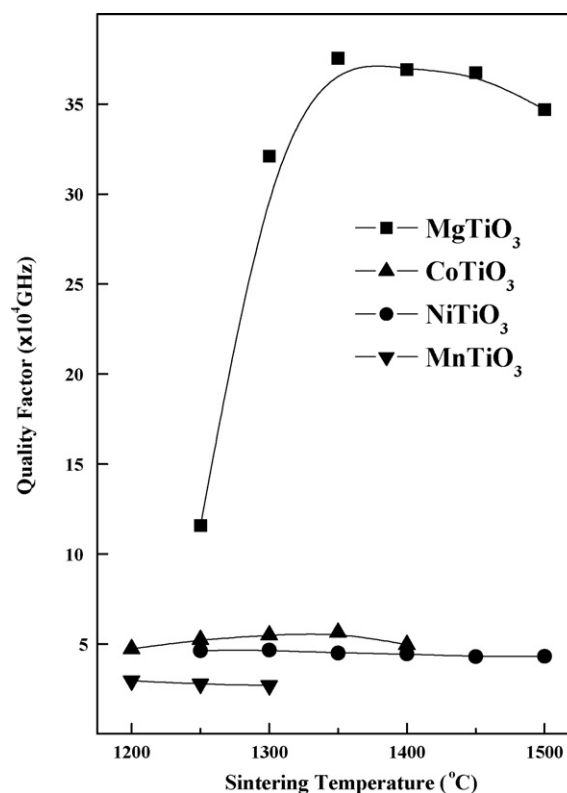


Fig. 5. Quality factor (Qf) value of ATiO_3 ($A = \text{Ni, Mg, Co, Mn}$) specimens sintered from 1200 to 1500 °C for 3 h.

Table 3

Average octahedral distortion and *TCF* of ATiO_3 ($A = \text{Ni, Mg, Co, Mn}$) sintered specimens.

	NiTiO_3	CoTiO_3	MgTiO_3	MnTiO_3
$R_{1\text{A-O}} (\text{\AA}) \times 3$	2.103	2.170	2.165	2.278
$R_{2\text{A-O}} (\text{\AA}) \times 3$	1.995	2.052	2.045	2.107
Average $R_{\text{A-O}} (\text{\AA})$	2.049	2.111	2.105	2.193
$R_{1\text{Ti-O}} (\text{\AA}) \times 3$	2.107	2.085	2.089	2.082
$R_{2\text{Ti-O}} (\text{\AA}) \times 3$	1.896	1.870	1.866	1.874
Average $R_{\text{Ti-O}} (\text{\AA})$	2.002	1.977	1.977	1.978
A-site octahedral distortion ($\Delta_{\text{A}} \times 10^3$)	0.698	0.785	0.821	1.520
Ti-site octahedral distortion ($\Delta_{\text{Ti}} \times 10^3$)	2.767	2.978	3.186	2.758
Average octahedral distortion ($\Delta \times 10^3$)	1.733	1.881	2.003	2.139
<i>TCF</i> (ppm/ $^{\circ}\text{C}$)	−48.48	−52.57	−54.48	−63.92

agreement with the change of grain size. Shon et al.¹³ reported that the *Qf* value of MgTiO_3 specimens was larger than those of the other ilmenite titanates due to the absence of 3d electrons which induce the conductivity.

Generally, Raman spectroscopy was used as an ideal tool for probing the degree of ordering. Raman modes move to higher frequencies for the well-ordered structures.¹⁴ Ten Raman active vibrational modes ($5A_g + 5E_g$) are predicted for the ilmenite structure.¹⁵ A_{1g} , E_{1g} and E_{2g} modes of ATiO_3 ($A = \text{Ni, Mg, Co, Mn}$) sintered specimens are shown in Fig. 6. With the types of A-site ions ($A = \text{Mn, Ni, Co, Mg}$), all of the modes move

to higher frequencies due to the increase of the A-site ordering. Therefore, the increase of *Qf* value with the A-site ions ($A = \text{Mn, Ni, Co, Mg}$) could be attributed to the increase of A-site ordering in ATiO_3 ilmenite structure.

Table 3 summarizes the average octahedral distortion and the temperature coefficient of resonant frequency (*TCF*) of ATiO_3 ($A = \text{Ni, Mg, Co, Mn}$) sintered specimens. The individual bond lengths of oxygen octahedra were obtained from the lattice parameters and atomic positions, as confirmed in Table 1. From the individual bond length of oxygen octahedra, the octahedral distortion was calculated by the equation reported by Shannon.² The octahedral distortion of A-site was smaller than that of Ti-site in entire compositions. With the increase of ionic radius of A-site ions ($A = \text{Ni, Co, Mg, Mn}$), the *TCF* of the specimens was decreased due to the increase of average octahedral distortion. These results that *TCF* of ATiO_3 ilmenite titanate depended on the octahedral distortion are also agreed with the reports of perovskite titanate.¹⁶

4. Conclusions

For the sintered specimens of ATiO_3 ($A = \text{Ni, Mg, Co, Mn}$), a single phase of ilmenite structure was confirmed through the entire composition. The dielectric constant (*K*) of ATiO_3 ($A = \text{Ni, Mg, Co, Mn}$) specimens was depended on the electronic oxide polarizabilities resulted from the energy gap and the molar volume as well as the polarizability of cation. The quality factor (*Qf*) of ATiO_3 ($A = \text{Co, Ni, Mn}$) specimens was appreciably lowered than that of MgTiO_3 specimens. These results could be attributed to the degree of average covalency of A–O and Ti–O bond, and the degree of A-site ordering confirmed by the shift of Raman mode. With the increase of ionic radius of A-site ions ($A = \text{Ni, Co, Mg, Mn}$), the *TCF* of the specimens was decreased due to the increase of average octahedral distortion.

Acknowledgment

This research was supported by Basic Science Research Program through the National Research Foundation of Korea (NRF) funded by the Ministry of Education, Science and Technology.

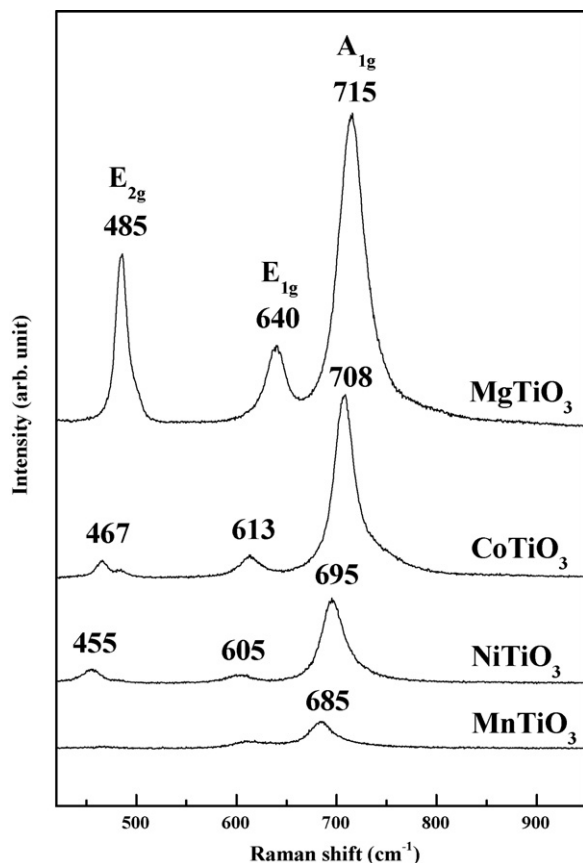


Fig. 6. Raman spectra of ATiO_3 ($A = \text{Ni, Mg, Co, Mn}$) sintered specimens.

References

1. Liferovich, R. P. and Mitchell, R. H., Geikielite–ecandrewsite solid solutions: synthesis and crystal structures of the $\text{Mg}_{1-x}\text{Zn}_x\text{TiO}_3$ ($0 \leq x \leq 0.8$) series. *Acta Cryst.*, 2004, **B60**, 496–501.
2. Shannon, R. D., Revised effective ionic radii and systematic studies of interatomic distances in halides and chalcogenides. *Acta Cryst.*, 1976, **A32**, 751–767.
3. Kuang, X., Jing, X. and Tang, Z., Dielectric loss spectrum of ceramic MgTiO_3 investigated by AC impedance and microwave resonator measurements. *J. Am. Ceram. Soc.*, 2006, **89**, 241–246.
4. Izumi, F. and Ikeda, T., A Rietveld-analysis program RIETAN-98 and its applications to zeolites. *Mater. Sci. Forum*, 2000, **321–324**, 198–203.
5. Wechsler, B. A. and Von Dreele, R. B., Structure refinements of Mg_2TiO_4 , MgTiO_3 and MgTi_2O_5 by time-of-flight neutron powder diffraction. *Acta Cryst.*, 1989, **B45**, 542–549.
6. Hakki, B. W. and Coleman, P. D., A dielectric resonator method of measuring inductive capacities in the millimeter range. *IRE Trans. Microwave Theory Tech.*, 1960, **8**, 402–410.
7. Nishikawa, T., Wakino, K., Tamura, H., Tanaka, H. and Ishikawa, Y., Precise measurement method for temperature coefficient of microwave dielectric resonator material. *IEEE MTT-S Int. Microwave Symp. Dig.*, 1987, **87**, 277–280.
8. Pauling, L., The nature of the chemical bond. IV. The energy of single bonds and the relative electronegativity of atoms. *J. Am. Chem. Soc.*, 1932, **54**, 3570–3582.
9. Brown, I. D. and Shannon, R. D., Empirical bond-strength-bond-length curves for oxides. *Acta Cryst.*, 1973, **A29**, 266–282.
10. Brown, I. D. and Wu, K. K., Empirical parameters for calculating cation–oxygen bond valences. *Acta Cryst.*, 1976, **B32**, 1957–1959.
11. Shannon, R. D., Dielectric polarizabilities of ions in oxides and fluorides. *J. Appl. Phys.*, 1993, **73**, 348–366.
12. Dimitrov, V. and Sakka, S., Electronic oxide polarizability and optical basicity of simple oxides. I. *J. Appl. Phys.*, 1996, **79**, 1736–1740.
13. Shon, J. H., Inaguma, Y., Yoon, S. O., Itoh, M., Nakamura, T., Yoon, S. J. and Kim, H. J., Microwave dielectric characteristics of ilmenite-type titanates with high Q values. *Jpn. J. Appl. Phys.*, 1994, **33**, 5466–5470.
14. Webb, S. J., Breeze, J., Scott, R. I., Cannell, D. S., Iddles, D. M. and Alford, N. M., Raman spectroscopic study of gallium-doped $\text{Ba}(\text{Zn}_{1/3}\text{Ta}_{2/3})\text{O}_3$. *J. Am. Ceram. Soc.*, 2002, **85**, 1753–1756.
15. Wang, A., Kuebler, K. E., Jolliff, B. L. and Haskin, L. A., Raman spectroscopy of Fe–Ti–Cr-oxides, case study: martian meteorite EETA79001. *Am. Mineral.*, 2004, **89**, 665–680.
16. Park, H. S., Yoon, K. H. and Kim, E. S., Relationship between the bond valence and the temperature coefficient of the resonant frequency in the complex perovskite $(\text{Pb}_{1-x}\text{Ca}_x)[\text{Fe}_{0.5}(\text{Nb}_{1-y}\text{Ta}_y)_{0.5}]\text{O}_3$. *J. Am. Ceram. Soc.*, 2001, **84**, 99–103.